State-selective preparation of Ar^{2+} and Kr^{2+} by resonantly enhanced two-photon double ionization via intermediate Rydberg states using high-order harmonics

Kana Yamada,[1] Atsushi Iwasaki,[1] Takahiro Sato,[1] Katsumi Midorikawa,[2] and Kaoru Yamanouchi[1,*]

[1]*Department of Chemistry, School of Science, The University of Tokyo, 7-3-1 Hongo, Bunkyo-ku, Tokyo 113-0033, Japan*

[2]*Attosecond Science Research Team, Extreme Photonics Research Group, RIKEN Center for Advanced Photonics, 2-1 Hirosawa, Wako-shi, Saitama 351-0198, Japan*

(Received 4 July 2016; revised manuscript received 10 September 2016; published 14 November 2016)

Simultaneous two-electron emission processes of Ar induced by high-order harmonics of near-infrared femtosecond laser pulses were investigated by coincidence photoelectron spectroscopy. Two-photon double ionization processes via the $3s3p^6np$ ($n \sim 25$) intermediate resonances of Ar were observed, which selectively created the $3s3p^5\,{}^1P$ state of Ar^{2+}. The similar double ionization processes were also observed in Kr. The selective creation indicates that the core electron configuration of the doubly ionized state tends to be the same as that of the intermediate state and that the emitted two electrons tend to form the singlet state.

DOI: 10.1103/PhysRevA.94.053414

I. INTRODUCTION

When atoms are photoionized by one-photon absorption, the resultant singly charged atomic ions are populated in the energetically allowed states and the population distribution among these states has been known to be close to their statistical weight [1]. However, in the case of the double photoionization, it has been known that the population distribution of the resultant doubly charged atomic ion can vary depending on the photoionization scheme [2–4], and in some cases, it can deviate largely from the statistical distribution [2,3]. The origin of such deviations from the statistical distribution in the double photoionization of atoms has been an attractive issue in recent decades [2–12].

For a one-photon threshold double ionization process of rare-gas atoms, it was theoretically predicted [5] that the population distribution of the doubly ionized states deviates to a large extent from the statistical distribution. The prediction called extended Wannier's law [5,13,14] tells us that the states of the resultant doubly charged atomic ion tend to be prepared so that a pair of electrons being emitted from the neutral atom takes all odd or all even L, S, and π, which represent, respectively, the total orbital angular momentum quantum number, the total spin angular momentum quantum number, and the parity. This tendency in the threshold double ionization processes was experimentally confirmed by detecting in coincidence two emitted electrons with near-zero kinetic energies [2]. However, the extended Wannier's law could not explain the population distribution when the excess energy becomes larger. Indeed, it was reported for Ar, Kr, and Xe that, when the excess energy was about 5 eV or more, the population in the $ns^2np^4\,{}^3P$ state was smaller than those expected from the statistical population distribution if the effect of the autoionization is taken into account [4].

It has been known that the population distribution can also be affected by the spin state of the emitted electron pair. The spin state of the emitted electron pair was investigated theoretically for the one-photon simultaneous two-electron emission processes of excited He($1s2s$) [6–9], ground-state Li($1s^22s$) [10,11], and excited Be($1s^22s2p$) [12]. The investigations were performed by the R-matrix method [6,10], the convergent close-coupling method [7,11], the time-dependent close-coupling method [8,10,11], the exterior complex scaling method [12], and a method in which a knockout process was treated quasiclassically and a shake-off process was treated quantum mechanically [9]. These studies consistently showed that the emitted electron pair tends to be in the singlet state, and this tendency was qualitatively interpreted by Pauli's exclusion principle [6,9]. The preference of the emission of the singlet electron pair was observed when spin-polarized He [15,16] and alkali-metal atoms [17,18] were ionized by the impact of a spin-polarized electron, but the preference in the double photoionization of rare-gas atoms has not been reported before to the best of our knowledge.

Recently, the double photoionization process induced by multiple photon absorption was investigated experimentally. Three-photon sequential double ionization of Ar was investigated by using an intense extreme ultraviolet free-electron laser [19–23]. In these studies, Ar^+ in the $3s^23p^5\,{}^2P_{3/2,1/2}$ levels were resonantly ionized by the absorption of additional two photons via the intermediate resonances of Ar^+. It was found that the population distribution in the resulting $3s^23p^4\,{}^3P$, ${}^1D$, and ${}^1S$ states of Ar^{2+} was significantly influenced by the choice of the intermediate resonance of Ar^+.

In the present study, we investigate double photoionization processes of Ar and Kr induced by the resonantly enhanced two-photon ionization using high-order harmonics of near-infrared laser pulses. The population distributions of Ar^{2+} and Kr^{2+} were found to be largely deviated from the statistical distributions. Indeed, only one of the energetically allowed states was prepared exclusively. On the basis of this finding we examine the role of the intermediate resonant states of Ar and Kr in determining the population distribution of the resultant Ar^{2+} and Kr^{2+}.

II. EXPERIMENT

High-order harmonics were generated by focusing Ti:sapphire laser pulses (~10 mJ, ~40 fs, 1 kHz, 795 nm) by a quartz lens ($f = 2$ m) into a 15-mm-long gas cell with a hole (1.5 mm ϕ) filled with an Ar gas. The Ar gas was introduced

*Corresponding author: kaoru@chem.s.u-tokyo.ac.jp

into the gas cell through a pulsed valve operated synchronously with the laser pulses. It was confirmed by a flat-field type extreme ultraviolet spectrometer that the high-order harmonics up to the 29th were generated. By using a calibrated photodiode (AXU100G, Opto Diode Co.), the intensity of the most intense 23rd harmonic was estimated to be ∼1 nJ/pulse.

The generated harmonics passed through two apertures of 6 and 3 mm diameters, which block the outer part of the copropagating fundamental laser beam having the divergence angle larger than that of the harmonics. The harmonics were reflected by two Si mirrors at the Brewster's angle of the fundamental light pulses (∼15°) in order to further reduce the intensity of the residual fundamental light pulses. The intensities of the residual fundamental light pulses and the ninth and lower-order harmonics became negligibly small after they passed through an Al filter whose thickness is 200 nm. Its transmittance is smaller than $\sim 10^{-6}$ for the fundamental light and the low-order harmonics in the wavelength range longer than 88 nm, while it is larger than 0.6 for the 13th and higher-order harmonics [24]. The 23rd and 25th harmonics were selected by using two SiC/Mg multilayered mirrors (NTT-AT Co.), having the reflectivities of 3, 5, 49, 19, and 3% at the incident angle of ∼2° for the 19th, 21st, 23rd, 25th, and 27th harmonics, respectively.

The selected harmonics propagated ∼10 mm below the interaction region in a magnetic-bottle type photoelectron spectrometer (FOM, Netherlands) [25], and were back focused onto the interaction region by a SiC/Mg multilayered concave mirror ($f = 150$ mm, NTT-AT Co.) at the incident angle of ∼2°. The polarization direction of the harmonics was parallel to the time-of-flight (TOF) axis. By recording a photoelectron spectrum of Xe irradiated with the selected harmonics, it was confirmed that the 9th through 27th harmonics were selected and that the intensities of the 23rd and 25th harmonics were two orders of magnitude larger than those of the rest of the harmonics. The total intensity of the harmonics at the interaction region was estimated to be in the range of 10^7–10^8 W/cm^2 by taking into account the reflectivities of the mirrors and the transmittance of the filter. A sample gas was continuously introduced through a needle whose inner diameter is 70 μm ϕ. The tip of the nozzle needle was placed ∼2 mm above the interaction region, and the focused harmonics crossed the sample atomic beam at right angles.

The photoelectrons emitted from the sample gas in the interaction region were introduced into the TOF tube through an aperture (2 mm ϕ), and were detected by a microchannel plate detector (PHOTONIS). The collection angle for photoelectrons was 2π sr. The signals were recorded by a data acquisition board (TDC8HP, RoentDek GmbH), and when two electrons were detected for one shot of harmonics, they were regarded as simultaneously emitted electrons. The signal count rate was kept below 0.3 counts/pulse in order to sufficiently reduce the number of false coincidence events. The energy axis of the recorded photoelectron spectra was calibrated by the photoelectron peaks originating from the $5p$ electron emissions from Xe induced by the 9th to 13th harmonics and by the 21st to 25th harmonics, such that the energy difference between the $5s^2 5p^5\ ^2P_{3/2}$ and $^2P_{1/2}$ levels of Xe^+ becomes close to 1.3064 eV [26]. The uncertainties in the calibrated electron kinetic energies were estimated to be ±4%. The full widths at half maximum of these peaks in the photoelectron spectra were ∼0.7 eV, which can be regarded as the energy resolution of the recorded photoelectron spectra. The photon energies of the harmonics were estimated from the calibrated energies of the photoelectron peaks assigned to the emissions of $5p$ electrons from Xe.

The photoelectron measurements of Ar were performed with the harmonics generated in two different conditions using the same experimental setup. In one condition, the Ar gas pressure at the harmonics-generation chamber was 2×10^{-2} Pa and the fundamental pulse energy was 10.3 mJ (condition 1), while in the other condition, the Ar gas pressure at the harmonics-generation chamber was 6×10^{-2} Pa and the fundamental pulse energy was 11.3 mJ (condition 2). In each condition, the distance between the gratings in the pulse compressor was adjusted so that the total intensities of the harmonics were maximized. The signals were accumulated for 3.3 h in condition 1 and for 8.3 h in condition 2. The coincidence photoelectron measurement of the double ionization of Kr was performed using harmonics generated in condition 1, and the accumulation time was 0.5 h.

III. RESULTS AND DISCUSSION

A. Relative intensities of harmonics

The 23rd and 25th harmonics induced one-photon single ionization of Ar through which one $3p$ electron is emitted, and two peaks originating from these processes were observed in the photoelectron spectra in the region between 18 and 25 eV in both cases when the harmonics were generated in condition 1 [Fig. 1(a)] and in condition 2 [Fig. 1(b)]. The spin-orbit splitting of the $3s^2 3p^5\ ^2P_{3/2,1/2}$ levels was not resolved because the energy separation of 0.18 eV [27] was smaller than the energy resolution (∼0.7 eV) of the measurements. The peak at 20.3 eV in condition 1 [Fig. 1(a)] and the peak at 19.8 eV in condition 2 [Fig. 1(b)] were assigned to the emission of a $3p$ electron induced by the 23rd harmonic, and the peak at 23.3 eV in condition 1 and the peak at 22.8 eV in condition 2 were assigned to the emission of a $3p$ electron induced by the 25th harmonic. The peak energies in condition 2 were smaller by ∼0.5 eV than those in condition 1 because the fundamental laser pulses were more positively chirped in condition 2 than in condition 1, and consequently, the harmonics were redshifted.

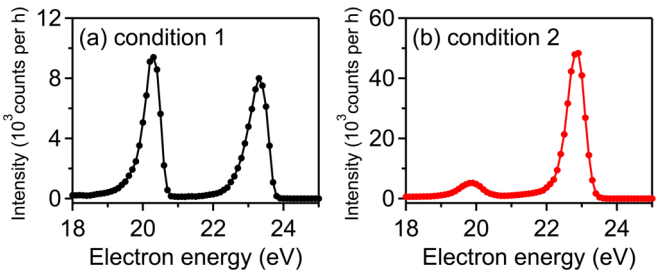

FIG. 1. Photoelectron spectra of Ar atoms obtained by the irradiation of the high-order harmonics generated in condition 1 (a) and condition 2 (b). Two peaks corresponding to the emission of a $3p$ electron by the 23rd and 25th harmonics are observed, respectively, at 20.3 ± 0.9 and 23.3 ± 1.1 eV in condition 1 and 19.8 ± 0.8 and 22.8 ± 1.0 eV in condition 2.

Although the photoelectron spectra in the lower energy region showed peaks assigned to the $3p$ electron emission induced by the 11th to 21st harmonics and the $3s$ electron emission induced by the 19th to 25th harmonics, they were about two orders of magnitude less intense than the peaks observed in Fig. 1.

The relative integrated intensity of the photoelectron peak associated with the creation of the $3s^2 3p^5\ ^2P$ state of Ar^+ by the 23rd harmonic to the corresponding peak produced by the 25th harmonic was 1.1 in condition 1, while it was 0.16 in condition 2. Because the relative cross section of the $3p$ electron emission induced by the 23rd harmonic to the $3p$ electron emission induced by the 25th harmonic is ~1.8 [28], the relative intensities of the 23rd harmonic to the 25th harmonic were estimated to be 0.6 in condition 1 and 0.09 in condition 2.

B. Two-photon double ionization processes

Correlation maps of the energies of the slow electrons (E_{slow}) and the fast electrons (E_{fast}) are plotted for condition 1, in which the intensities of the 23rd and 25th harmonics are comparable [Fig. 2(a)], and condition 2, in which the intensity of the 25th harmonic dominates [Fig. 2(b)]. Figure 2(a) exhibits two lines whose slope is −1.0, and Fig. 2(b) exhibits one line whose slope is −1.0. These lines indicate that the excess photon energies for double ionizations are distributed between two electrons emitted simultaneously. The excess photon energies in these processes appear as the peaks in the distribution of the total kinetic energies of the slow and fast electrons detected in coincidence [Figs. 2(c) and 2(d)]. Figure 2(c) shows that the excess photon energies are 4.48 and 7.42 eV in condition 1, and Fig. 2(d) shows that the excess photon energy was 6.94 eV in condition 2.

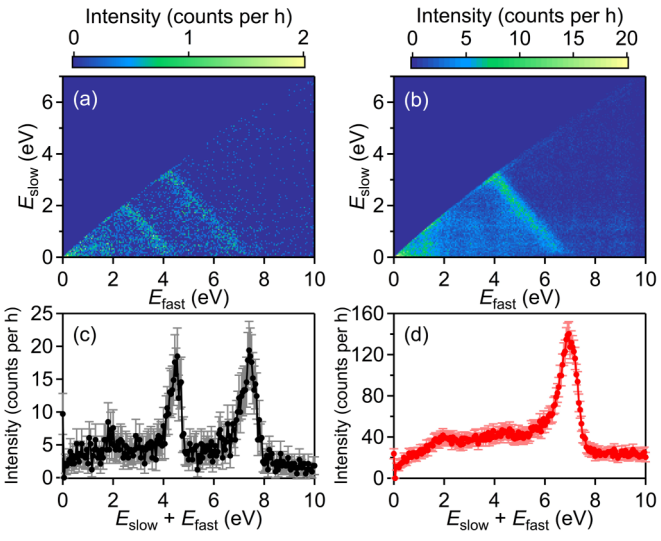

FIG. 2. Correlation maps of two electrons ejected from Ar atoms [(a), (b)] and total energy distributions of the correlated electrons [(c), (d)]. The spectra were obtained by the irradiation of the high-order harmonics generated in condition 1 [(a), (c)] and condition 2 [(b), (d)]. Signals were not detected when the energies of E_{fast} and E_{slow} were close because the data acquisition board could not separate the TOF of these electrons. The peaks in (c) and (d) correspond to the diagonal line-shaped structures in (a) and (b), respectively.

The distributions of the total kinetic energies in Figs. 2(c) and 2(d) look very similar to the photoelectron spectra in Figs. 1(a) and 1(b), respectively. The similarity indicates that the 23rd harmonic contributes to the simultaneous two-electron emission process with the excess energy of 4.48 eV observed in condition 1 (process I), and the 25th harmonic contributes to the processes with the excess energy of 7.42 eV in condition 1 and 6.94 eV in condition 2 (process II). These processes are multiphoton processes because the double ionization threshold energy of Ar (43.39 eV [26]) is higher than the photon energies of the 23rd and 25th harmonics. Because the energy difference between the two peaks observed in Fig. 2(c) corresponded to the energy difference between the 23rd and 25th harmonics, the additional photon energy should be common in these processes. The energy of the additional photon is expected to be in resonance with an energy of an excited state of Ar because a multiphoton process can be realized only when there is resonance enhancement at the weak intensities of the harmonics (10^7–10^8 W/cm^2), which is four orders of magnitude weaker than the intensities in the previous studies on the two-photon nonresonant double ionization processes of Ar [29,30].

The sum of the energy of the additional photon, E_{res}, for achieving the resonance enhancement and the photon energy of the high-order harmonic is equal to the sum of the energy of the resultant state of Ar^{2+}, $E(Ar^{2+})$ and the total kinetic energy of the two electrons E_{2e}(=E_{slow} and E_{fast}) ejected upon the double ionization, that is,

$$E_{res} + h\nu(23\text{rd}) = E(Ar^{2+}) + E_{2e}(\text{I}) \quad (1)$$

holds for process I, where $h\nu$(23rd) denotes the photon energy of the 23rd harmonic, and

$$E_{res} + h\nu(25\text{th}) = E(Ar^{2+}) + E_{2e}(\text{II}) \quad (2)$$

holds for process II, where $h\nu$(25th) denotes the photon energy of the 25th harmonic. It is found that these two equations are fulfilled when E_{res} corresponds to the photon energy of the 19th harmonic (29.2 eV in condition 1 and 29.5 eV in condition 2) with which Ar^{2+} is prepared either in the $3s3p^5\ ^1P$ state or in the $3s^2 3p^3 3d\ ^5D$ state of Ar^{2+} (Table I). It is also found that the photon energy of the 19th harmonic coincides with the $3s3p^6np$ ($n \sim 25$) Rydberg states of Ar, which converge to the $3s3p^6\ ^2S_{1/2}$ level of Ar^+ (29.24 eV) [26], therefore the 19th harmonic can contribute to the ionization process even though its intensity is much weaker than the intensities of the 23rd and 25th harmonics, and the two-photon process is realized.

The $3s3p^6np$ Rydberg states of Ar are considered to be the ^1P states so that it is accessed from the ground ^1S state of Ar by one-photon absorption. The mixing with other configurations is considered to be small because the configuration mixing is known to be negligibly small [31]. As for Ar^{2+}, as long as the total spin angular momentum in the double ionization process is conserved, the ^5D state of Ar^{2+} could not be created. Therefore, as shown in Fig. 3, it is highly probable that the double ionization is resonantly enhanced and proceeds as

$$\text{Ar}(3s^2 3p^6, {}^1S) + h\nu(19\text{th}) \rightarrow \text{Ar}^*(3s3p^6np, {}^1P), \quad (3)$$

$$\text{Ar}^*(3s3p^6np, {}^1P) + h\nu(23\text{rd or } 25\text{th}) \rightarrow \text{Ar}^{2+}(3s3p^5, {}^1P) + 2e^-. \quad (4)$$

TABLE I. Derivation of E_{res} for each double ionization process of Ar.

Ar^{2+} state	$E(Ar^{2+})$ (eV)[a]	condition	$h\nu$ (eV)[b]	E_{2e}(eV)	E_{res}(eV)[c]
$^1P(3s3p^5)$	61.25	1	36.1	4.48	29.6
			39.1	7.42	29.6
		2	38.6	6.94	29.6
$^5D(3s^23p^33d)$	61.35	1	36.1	4.48	29.7
			39.1	7.42	29.7
		2	38.6	6.94	29.7

[a]Reference [26].
[b]Energies derived from Fig. 1 assuming that the first ionization potential of Ar is 15.8 eV [26]. The photon energies of 36.1 and 39.1 eV correspond, respectively, to the photon energies of the 23rd and 25th harmonics generated in condition 1, and the photon energy of 38.6 eV corresponds to the photon energy of the 25th harmonic generated in condition 2.
[c]Derived from Eqs. (1) and (2).

Although the total photon energies of the 19th + 23rd and 19th + 25th harmonics are sufficiently high for the creation of the other lower lying states of Ar^{2+} (see Fig. 3), no other lines with a slope of −1.0 can be identified in the higher energy region of the correlation maps, Figs. 5(a) and 5(b) in the Appendix. As explained in the Introduction, some deviations from the statistical population distribution of the resultant electronic states of doubly charged atoms upon the double photoionization have been reported before [2–5,19–23]. Unlike these reported processes, the observed process showed the exclusive preparation of doubly charged atoms in only one single electric state.

C. Anomalous selectivity

In the ionization of the excited $Ar^*(3s3p^6np)$ $(n \sim 25)$ to $Ar^{2+}(3s3p^5)$, one np and one of the $3p$ electrons are emitted. On the other hand, in the ionization of the excited

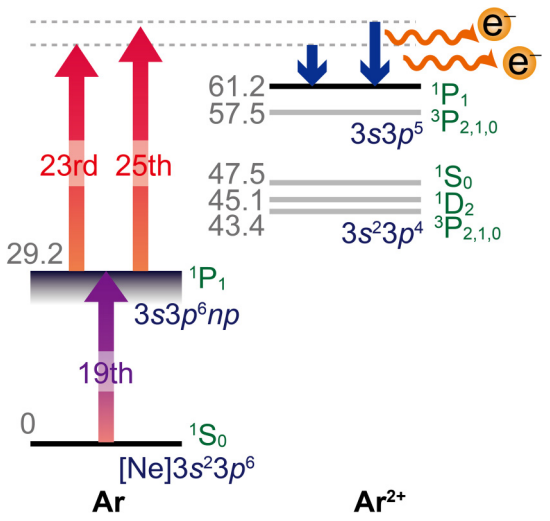

FIG. 3. Probable route of the observed double ionization process of Ar. The 19th harmonic excites Ar to the Rydberg states, and the 23rd or 25th harmonic induces a simultaneous two-electron emission to create the $3s3p^5\ ^1P_1$ level of Ar^{2+}. The energies from the ground state of Ar to the $3s^23p^4\ ^3P_2, ^1D_2, ^1S_0$ levels and the $3s3p^5\ ^3P_2, ^1P_1$ levels of Ar^{2+} and the $3s3p^6\ ^2S_{1/2}$ level of Ar^+ are shown in the unit of eV.

Ar to $Ar^{2+}(3s^23p^4)$, one of the $3p$ electrons relaxes to the $3s$ orbital in addition to the emissions of np and $3p$ electrons. The selective creation of $Ar^{2+}(3s3p^5)$ suggests that the double ionization proceeds with the minimum changes in the electron configuration from that of the resonance intermediate state. The changes in the electron configuration in the single photoionization process is discussed by using Dyson norm [32], which is defined as the overlap integral between the wave functions of the initial and singly ionized states. It has been known that the Dyson norm becomes large when the core electron configuration is kept upon the ionization. Because the single ionization probability is proportional to the Dyson norm, the dominant ionization process has the minimum electron configuration changes. Our observation indicates that this propensity of the minimum configuration change in single ionization processes can also be applied to the double ionization from the $3s3p^6np$ $(n \sim 25)$ excited Ar.

Within the LS scheme, the total spin angular momentum of Ar is conserved through the double ionization process as

$$\mathbf{S}_{int} = \mathbf{S}_{ion} + \mathbf{S}_{e-e}, \tag{5}$$

where $\mathbf{S}_{int}$, $\mathbf{S}_{ion}$, and $\mathbf{S}_{e-e}$ are the spin angular momenta of the intermediate excited state, the doubly ionized state, and the electron pair, respectively. Because both the intermediate excited Ar and the created Ar^{2+} are in the singlet states, which means $S_{int} = S_{ion} = 0$, the emitted electron pair should be in the singlet state, that is, $S_{e-e} = 0$.

The observed two-electron emissions are achieved by the one-photon excitation from the excited $Ar^*(3s3p^6np)$, in which one electron is promoted to the outermost orbital. One-photon double ionizations of atoms having this type of configuration such as excited $He(1s2s)$ [6–9], ground-state $Li(1s^22s)$ [10,11], and excited $Be(1s^22s2p)$ [12] have been theoretically studied. In these studies, the cross section of the emission of a triplet electron pair is always smaller than the cross section of the emission of a singlet electron pair, and this propensity for the emission of the singlet pair was interpreted by the Pauli's exclusion principle explaining the smaller correlation between the electrons in a triplet pair. In the double photoionization of the ground state of Li, the cross section of the singlet electron pair emission was calculated to be 2.7 times larger than that of the triplet electron pair emission at the excess energy of 5 eV [10]. Our observation showed that

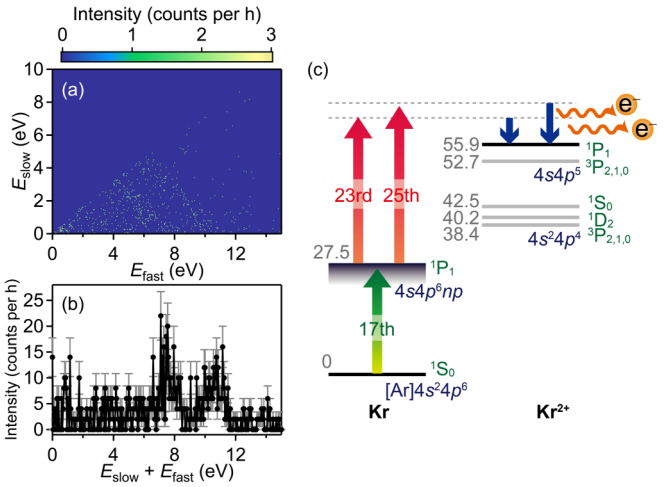

FIG. 4. Correlation maps of two electrons ejected from Kr (a), the total energy distribution of the correlated electrons (b), and probable route of the observed double ionization process (c). The spectra were observed by the irradiation of the harmonics generated in condition 1. In the observed process, the 17th harmonic excites Kr to the Rydberg states, and the 23rd or 25th harmonic induces a simultaneous two-electron emission to create the $4s4p^5\,{}^1P_1$ level of Kr^{2+}. The energies from the ground state of Kr to the $4s^24p^4\,{}^3P_2, {}^1D_2, {}^1S_0$ levels and the $4s4p^5\,{}^3P_2, {}^1P_1$ levels of Kr^{2+} and the $4s4p^6\,{}^2S_{1/2}$ level of Kr^+ are shown in the unit of eV.

the singlet electron pair emission occurs exclusively in the one-photon double ionization of the excited $Ar^*(3s3p^6np)$. It seems that the emitted electron pair tends to be in the singlet state in the one-photon double ionization of atoms having the configuration in which one electron is in the outermost orbital.

D. Double ionization of Kr

In a similar manner introduced above for the double ionization of Ar, we investigated the double ionization of Kr by the irradiation of the high-order harmonics of near-infrared laser pulses generated in condition 1. In condition 1, the intensities of the 23rd and 25th harmonics were comparable, and two lines exhibiting a slope of -1.0 are observed in the correlation map below 15 eV as shown in Fig. 4(a). No other lines were observed in the higher energy region. The sums of the energies of the simultaneously emitted electrons were 7.57 and 10.58 eV as seen in Fig. 4(b), which indicate that the excess energy is 7.57 eV when the 23rd harmonic contributes to the simultaneous two-electron emission process (process I′) and the excess energy is 10.58 eV when the 25th harmonic contributes to the emission process (process II′).

From the energy conservation, in a similar manner as in the case of Ar,

$$E_{res} + h\nu(23rd) = E(Kr^{2+}) + E_{2e}(I') \quad (6)$$

holds for process I′, and

$$E_{res} + h\nu(25th) = E(Kr^{2+}) + E_{2e}(II') \quad (7)$$

holds for process II′. The photon energies, $h\nu$(23rd) and $h\nu$(25th), are those derived from the photoelectron spectrum of Ar in Fig. 1(a). It is found that these two equations are approximately fulfilled (i) when E_{res} corresponds to the photon energy of the ninth harmonic (14.1 eV in condition 1) and the $4s^24p^4\,{}^1S$ state of Kr^{2+} is prepared or (ii) when E_{res} corresponds to the photon energy of the 17th harmonic (26.6 eV in condition 1) and the $4s4p^5\,{}^1P$ state or the $4s^24p^34d\,{}^5D$ state of Kr^{2+} is prepared (Table II). It is also found that (i) the photon energy of the ninth harmonic coincides with the $4s^24p^5nd$ ($n \sim 20$) Rydberg states of Kr and (ii) the photon energy of the 17th harmonic coincides with the $4s4p^6np$ ($n \sim 7$) Rydberg states of Kr converging to the $4s4p^6\,{}^2S_{1/2}$ level of Kr^+ (27.5 eV) [26].

TABLE II. Derivation of E_{res} for each double ionization process of Kr.

Kr^{2+} state	$E(Kr^{2+})$ (eV)[a]	$h\nu$ (eV)[b]	E_{2e}(eV)	E_{res}(eV)[c]
$^1S(4s^24p^4)$	42.46	36.1	7.57	13.9
		39.1	10.58	13.9
$^5D(4s^24p^34d)$	55.54	36.1	7.57	27.0
		39.1	10.58	27.0
$^1P(4s4p^5)$	55.95	36.1	7.57	27.4
		39.1	10.58	27.4

[a]Reference [26].
[b]Energies derived from Fig. 1 assuming that the first ionization potential of Ar is 15.8 eV [26]. The photon energies of 36.1 and 39.1 eV correspond, respectively, to the photon energies of the 23rd and 25th harmonics generated in condition 1.
[c]Derived from Eqs. (6) and (7).

However, in the current experimental conditions, the intensity of the ninth harmonic at the interaction point is estimated to be smaller than the intensity of the 17th harmonic by one order of magnitude. Therefore, it is more probable that the resonance enhancement is achieved by the 17th harmonic. In addition, as long as the LS scheme is assumed, the preparation of the $4s^24p^34d\,{}^5D$ state of Kr^{2+} is less likely because of the conservation of the total spin angular momentum under the LS scheme [33].

Therefore, as shown in Fig. 4(c), it is probable that the double ionization of Kr is resonantly enhanced and proceeds as

$$Kr(4s^24p^6, {}^1S) + h\nu(17th) \rightarrow Kr^*(4s4p^6np, {}^1P), \quad (8)$$

$$Kr^*(4s4p^6np, {}^1P) + h\nu(23rd\ or\ 25th) \rightarrow Kr^{2+}(4s4p^5, {}^1P) + 2e^-. \quad (9)$$

It should be noted that $E_{res} = 27.4$ eV, obtained from Eq. (6), or equivalently from Eq. (7), is larger than the photon energy of the 17th harmonic (26.6 eV) by 0.8 eV. Therefore, the resonance is considered to be achieved by the high energy tail of the 17th harmonic, and the selective preparation of the doubly charged atomic state is realized in Kr by the resonantly enhanced two-photon double ionization in almost the same manner as in Ar.

IV. SUMMARY

The coincidence photoelectron measurements revealed the selective creation of the $3s3p^5\,{}^1P$ state of Ar^{2+} through a

resonantly enhanced two-photon double ionization of Ar via the $3s3p^6np\,(n \sim 25)$ Rydberg states. In addition, a similar propensity was suggested in the two-photon double ionization of Kr, in which the $4s4p^5\,{}^1P$ state of Kr^{2+} was selectively prepared through a resonantly enhanced two-photon double ionization of Kr via the $4s4p^6np\,(n \sim 15)$ Rydberg states. In the observed processes, it was suggested that the core electron configuration did not change when the excited neutral Ar and Kr are doubly ionized, and all the emitted electron pairs are in the singlet state. Our observation suggested that the one-photon double ionization of an excited rare-gas atom with the $msmp^6np$ electron configuration shows a unique selectivity, and the process can be an attractive target for theoretical studies of the electron correlations in a many-electron system.

ACKNOWLEDGMENTS

This work was supported by JSPS Strategic Fund for Strengthening Leading-Edge Research and Development, JSPS KAKENHI Grants No. 19002006, No. 15H05696, and No. 24245003.

APPENDIX: CORRELATION MAPS OF Ar IN HIGHER ENERGY REGION

The correlation maps of the slow electrons whose energy $E_{\rm slow}$ is below 21 eV and the fast electrons whose energy $E_{\rm fast}$ is below 30 eV are plotted in Fig. 5. Figures 5(a) and 5(b) were obtained in condition 1 and condition 2, respectively. Figure 5(a) exhibits the vertical distributions at $E_{\rm fast} = 14.0, 15.7, 20.4$, and 23.3 eV. The two vertical lines observed at 20.4 and 23.3 eV are assigned to false coincidence events between a slower electron and a $3p$ electron emitted after the single ionization by the 23rd and 25th harmonics. The two vertical lines at 14.0 and 15.7 eV are assigned to the ringing signals appearing $\sim$36 μs after the false coincidence signals. In a similar manner, in Fig. 5(b), the two vertical lines at 19.9 and 22.9 eV are the false coincidence signals, and the two vertical lines at 13.8 and 15.6 eV are their ringing signals.

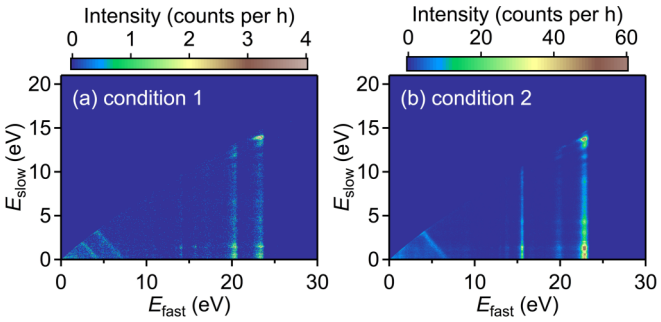

FIG. 5. Correlation maps of two electrons emitted from Ar obtained by the irradiation of the high-order harmonics generated in condition 1 (a) and condition 2 (b).

[1] J. H. D. Eland, *Photoelectron Spectroscopy* (Butterworths, London, 1974).
[2] R. I. Hall, G. Dawber, A. G. McConkey, M. A. MacDonald, and G. C. King, Z. Phys. D **23**, 377 (1992).
[3] B. Möbus, K.-H. Schartner, A. Ehresmann, and H. Schmoranzer, Z. Phys. D **30**, 285 (1994).
[4] J. H. D. Eland, O. Vieuxmaire, T. Kinugawa, P. Lablanquie, R. I. Hall, and F. Penent, Phys. Rev. Lett. **90**, 053003 (2003).
[5] A. Huetz, P. Selles, D. Waymel, and J. Mazeau, J. Phys. B **24**, 1917 (1991).
[6] H. W. van der Hart, K. W. Meyer, and C. H. Greene, Phys. Rev. A **57**, 3641 (1998).
[7] A. S. Kheifets, A. Ipatov, M. Arifin, and I. Bray, Phys. Rev. A **62**, 052724 (2000).
[8] J. Colgan and M. S. Pindzola, Phys. Rev. A **67**, 012711 (2003).
[9] A. Emmanouilidou, T. Schneider, and J.-M. Rost, J. Phys. B **36**, 2717 (2003).
[10] J. Colgan, D. C. Griffin, C. P. Ballance, and M. S. Pindzola, Phys. Rev. A **80**, 063414 (2009).
[11] A. S. Kheifets, D. V. Fursa, C. W. Hines, I. Bray, J. Colgan, and M. S. Pindzola, Phys. Rev. A **81**, 023418 (2010).
[12] F. L. Yip, C. W. McCurdy, and T. N. Rescigno, Phys. Rev. A **81**, 063419 (2010).
[13] A. D. Stauffer, Phys. Lett. A **91**, 114 (1982).
[14] C. H. Greene and A. R. P. Rau, J. Phys. B **16**, 99 (1983).
[15] M. J. Alguard, V. W. Hughes, M. S. Lubell, and P. F. Wainwright, Phys. Rev. Lett. **39**, 334 (1977).
[16] G. Baum, M. Fink, W. Raith, H. Steidl, and J. Taborski, Phys. Rev. A **40**, 6734 (1989).
[17] G. Baum, W. Blask, P. Freienstein, L. Frost, S. Hesse, W. Raith, P. Rappolt, and M. Streun, Phys. Rev. Lett. **69**, 3037 (1992).
[18] G. Baum, M. Moede, W. Raith, and W. Schröder, J. Phys. B **18**, 531 (1985).
[19] A. N. Grum-Grzhimailo, E. V. Gryzlova, S. Fritzsche, and N. M. Kabachnik, J. Mod. Opt. **63**, 334 (2016).
[20] Y. Hikosaka, M. Fushitani, A. Matsuda, C.-M. Tseng, A. Hishikawa, E. Shigemasa, M. Nagasono, K. Tono, T. Togashi, H. Ohashi, H. Kimura, Y. Senba, M. Yabashi, and T. Ishikawa, Phys. Rev. Lett. **105**, 133001 (2010).
[21] N. Miyauchi, J. Adachi, A. Yagishita, T. Sako, F. Koike, T. Sato, A. Iwasaki, T. Okino, K. Yamanouchi, K. Midorikawa, K. Yamakawa, F. Kannari, H. Nakano, M. Nagasono, K. Tono, M. Yabashi, T. Ishikawa, T. Togashi, H. Ohashi, H. Kimura, and Y. Senba, J. Phys. B **44**, 071001 (2011).
[22] H. Fukuzawa *et al.*, J. Phys. B **43**, 111001 (2010).
[23] E. V. Gryzlova *et al.*, Phys. Rev. A **84**, 063405 (2011).
[24] B. L. Henke, E. M. Gullikson, and J. C. Davis, At. Data Nucl. Data Tables **54**, 181 (1993).
[25] P. Kruit and F. H. Read, J. Phys. E **16**, 313 (1983).
[26] A. Kramida, Yu. Ralchenko, J. Reader, and NIST ASD Team, *NIST Atomic Spectra Database (ver. 5.2), (online)* (National Institute of Standards and Technology, Gaithersburg, MA, 2014).
[27] E. B. Saloman, J. Phys. Chem. Ref. Data **39**, 033101 (2010).

[28] K.-N. Huang, W. R. Johnson, and K. T. Cheng, At. Data. Nucl. Data Tables **26**, 33 (1981).

[29] E. P. Benis, D. Charalambidis, T. N. Kitsopoulos, G. D. Tsakiris, and P. Tzallas, Phys. Rev. A **74**, 051402(R) (2006).

[30] K. Furusawa, T. Okino, T. Shimizu, H. Hasegawa, Y. Nabekawa, K. Yamanouchi, and K. Midorikawa, Appl. Phys. B **83**, 203 (2006).

[31] R. P. Madden, D. L. Ederer, and K. Codling, Phys. Rev. **177**, 136 (1969).

[32] M. Spanner, S. Patchkovskii, C. Zhou, S. Matsika, M. Kotur, and T. C. Weinacht, Phys. Rev. A **86**, 053406 (2012).

[33] D. L. Ederer, A. C. Parr, J. B. West, D. Holland, and J. L. Dehmer, Phys. Rev. A **25**, 2006 (1982).